Proc. Estonian Acad. Sci. Chem., 2000, **49**, 1, 53–70
https://doi.org/10.3176/chem.2000.1.06

MODELLING SO_2 CAPTURE BY ESTONIAN LIMESTONES AND DOLOMITES

Andres TRIKKEL[a], Ron ZEVENHOVEN[b], and Rein KUUSIK[a]

[a] Department of Basic and Applied Chemistry, Tallinn Technical University, Ehitajate tee 5, 19086 Tallinn, Estonia; atrik@edu.ttu.ee
[b] Department of Chemical Engineering, Åbo Akademi University, Lemminkäisenkatu 14-18B, FIN-20520, Åbo/Turku, Finland

Received 19 November 1999, in revised form 6 December 1999

Abstract. Sulphation of several chemically and physically different Estonian limestone and dolomite samples was studied by thermogravimetric analysis, accompanied by Hg-porosity, X-ray, and SEM measurements. The SO_2 binding capacity of the samples (particle size 125–160 μm) was analysed isothermally at 850 °C and at 1 or 15 bar in a gas mixture of 4% O_2, 15% CO_2, 0.5% SO_2, and N_2. The final values of conversion under these conditions were in the range of 32–66%, the amount of bound SO_2 being 15.5–34 mg per 100 mg of initial sample. An attempt was made to apply an unreacted shrinking core model with variable effective diffusivity to the CaO and $CaCO_3$ sulphation data under atmospheric and pressurized conditions. The rate parameters were calculated for the sulphation reaction and the limiting stages for the binding process were established.

Key words: sulphur binding, thermogravimetric analysis, flue gas desulphurization.

INTRODUCTION

Natural carbonaceous rocks such as limestone ($CaCO_3$) and dolomite ($CaCO_3 \cdot MgCO_3$) are widely used as relatively cheap sorbents for SO_2 removal from flue gases. Electricity in Estonia is generated almost completely by combustion of pulverized oil shale resulting in annual SO_2 emissions of up to 90 000 tonnes. At the same time, the sulphur capture ability of Estonian limestones and dolomites (consumption reserve 121 and 32 million m^3, respectively [1]) is high [2], but their application in flue gas desulphurization processes is largely unexplored.

At atmospheric pressure the sulphur binding process involves two steps. First, calcium carbonate in limestone decomposes to give calcium oxide and, after that, the formed CaO reacts with SO_2 to form $CaSO_4$ according to the summary Eq. 2:

$$CaCO_3 \leftrightarrows CaO + CO_2, \quad (1)$$

$$CaO + SO_2 + 1/2O_2 \leftrightarrows CaSO_4. \quad (2)$$

Diffusion of SO_2 through the formed $CaSO_4$ layer has been reported to be the rate limiting stage of this process [3, 4].

At pressurized conditions the binding process proceeds in one step and calcium carbonate reacts directly with SO_2 :

$$CaCO_3 + SO_2 + 1/2O_2 \leftrightarrows CaSO_4 + CO_2. \quad (3)$$

In this case the release of CO_2 takes place simultaneously with the reaction by SO_2 [5, 6].

The magnesium carbonate in dolomite decomposes both at atmospheric and pressurized conditions:

$$CaCO_3 \cdot MgCO_3 \leftrightarrows CaO + MgO + 2CO_2 \quad \text{(full calcination)}, \quad (4)$$

$$CaCO_3 \cdot MgCO_3 \leftrightarrows CaCO_3 + MgO + CO_2 \quad \text{(half calcination)}. \quad (5)$$

According to several authors the formed MgO shows no or very little absorption of SO_2 at temperatures above 800–850 °C due to thermodynamic limitations [7, 8].

Several mathematical models have been proposed to describe the sulphation process of single sorbent particles [9–12]. We used an unreacted shrinking core (USC) model with variable effective diffusivity [13–15] to determine rate parameters of reaction kinetics, mass transfer, and diffusion. This method has been earlier used for modelling sulphation and sulphidation of calcium-based sorbents at elevated pressures [13, 14].

In the present work different Estonian limestones and dolomites were investigated in order to get a comparative ranking of the sorbents using the extended USC model, both at atmospheric and pressurized conditions.

MATERIALS AND METHODS

Sulphation of several physically and chemically different Estonian limestone and dolomite samples was studied with a pressurized thermogravimetric device (DMT, Germany) [6, 13–15]. SO_2 binding by the samples (particle size 125–160 μm) was carried out isothermally at 850 °C and at 1 or 15 bar in the gas mixture of 4% O_2, 15% CO_2, 0.5% SO_2, and N_2. Dilution of 50 mg of the sample with 250 mg of quartz and a special cylindrical sample holder were used to diminish the sample bed and gas film diffusion. The gas flow in the experiments was 1.5 L/min (STP) for the runs at atmospheric pressure and 3 L/min for pressurized experiments, the diameter of the furnace tube being

12.5 mm. In the atmospheric runs the initial samples were heated to the experiment temperature in an SO_2-free gas mixture, calcined until the weight stabilized (both $CaCO_3$ and $MgCO_3$ decomposed), after which SO_2 was added to the gas mixture. In the pressurized runs, the initial material was heated up to the experiment temperature in 100% of CO_2 (only $MgCO_3$ decomposed), after which the composition of the gas mixture was adjusted.

The limestone and dolomite samples were selected so that a large variety in chemical composition (pure samples and with high impurities content) and structural characteristics (specific surface area, porosity, and pore distribution) could be achieved. The chemical composition and some physical properties of the samples used in these experiments are presented in Tables 1 and 2.

Table 1. Chemical composition of the samples (L = limestone, D = dolomite)

Sample (Deposit)	Content, %						
	CO_2	CaO	$CaCO_3$	$MgCO_3$	Insoluble residue	Fe_2O_3	Al_2O_3
Rummu L	40.98	54.93	92.26	0.80	0.49	0.18	0.05
Aseri L*	29.12	42.70	64.64	1.34	5.16	8.34	1.88
Harku L	35.50	45.10	78.80	1.63	10.57	0.68	10.20
Karinu L	40.44	50.60	86.93	4.25	3.85	0.34	0.16
Tamsalu L	43.16	42.02	68.28	25.16	1.51	0.30	0.62
Volkhov L*	35.00	43.76	76.47	2.64	15.47	0.73	0.84
Adavere D	42.75	28.82	46.68	42.57	4.34	0.50	0.30
Pajusi D	35.08	24.46	35.72	37.11	18.98	0.90	0.52
Koguva D	38.34	25.28	41.27	38.68	14.41	0.95	1.10
Hellamaa D	46.70	30.84	52.36	45.35	0.44	0.61	0.01

* Obtained from different layers of the Maardu deposit.

Table 2. Physical properties of the samples (L = limestone, D = dolomite)

Sample (Deposit)	Specific surface area, m^2/g		$\rho_{particle}$, kg/m^3	ε_0	S_{v0}, m^2/cm^3	d_{av}, μm
	Initial	Calcined*				
Rummu L	0.70	5.00	2902	0.28	2.33	0.470
Aseri L	13.17	3.90	2923	0.18	14.79	0.0461
Harku L	4.58	4.56	2619	0.15	11.35	0.0487
Karinu L	1.14	10.00	2681	0.09	3.62	0.0998
Tamsalu L	0.87	15.48	2816	0.04	1.00	0.176
Volkhov L	4.15	4.85	2685	0.13	5.46	0.0923
Adavere D	0.52	20.57	2801	0.07	1.33	0.206
Pajusi D	2.34	10.53	2761	0.21	4.06	0.204
Koguva D	7.19	9.56	2801	0.13	10.59	0.0498
Hellamaa D	0.34	22.18	3002	0.05	2.76	0.0792

* Obtained from separate calcination tests: 30 min at 900 °C in air, sample weight 1.0 g.

In this paper, all the parameters for calcined samples used were calculated on the basis of initial data for the raw samples and not obtained from separate calcination tests carried out in different conditions, as in our previous paper [15].

The volume of a sorbent particle before calcination can be expressed as follows:

$$Vol_{MgCO_3} + Vol_{CaCO_3} + Vol_{other} + Vol_{pores,0} = Vol_{particle}. \quad (6)$$

After calcination at atmospheric pressure we get

$$Vol_{MgO} + Vol_{CaO} + Vol_{other} + Vol_{pores,1} = Vol_{particle}, \quad (7)$$

which gives, assuming that the volume of the particle does not change

$$\varepsilon_1 = \varepsilon_0 + \frac{Vol_{MgCO_3}}{Vol_{particle}}\left(1 - \frac{Vol_{MgO}}{Vol_{MgCO_3}}\right) + \frac{Vol_{CaCO_3}}{Vol_{particle}}\left(1 - \frac{Vol_{CaO}}{Vol_{CaCO_3}}\right), \quad (8)$$

where $Vol_{MgO}/Vol_{MgCO_3} = 11.26\ cm^3\ mol^{-1}/28.51\ cm^3\ mol^{-1} = 0.395$;

$Vol_{CaO}/Vol_{CaCO_3} = 16.9/36.9 = 0.458$ according to their molar volume ratios, and

$$\frac{Vol_{MgCO_3}}{Vol_{particle}} = \frac{\%MgCO_3\,\rho_{particle}}{100\rho_{MgCO_3}}, \qquad \frac{Vol_{CaCO_3}}{Vol_{particle}} = \frac{\%CaCO_3\,\rho_{particle}}{100\rho_{CaCO_3}}. \quad (9)$$

Under elevated pressure (only $MgCO_3$ decomposes) we get

$$\varepsilon_1 = \varepsilon_0 + \frac{Vol_{MgCO_3}}{Vol_{particle}}\left(1 - \frac{Vol_{MgO}}{Vol_{MgCO_3}}\right). \quad (10)$$

The pore surface area after calcination, S_{v1}, was estimated by

$$\frac{S_{v0}^2}{S_{v1}^2} = \frac{\varepsilon_0}{\varepsilon_1} \quad (11)$$

and the average pore radius was obtained from

$$r_{av} = \frac{2\varepsilon_1}{S_{v1}}, \quad (12)$$

assuming that pores are identical cylinders.

Calculated structural properties of the sorbent samples are presented in Table 3. The initial porosities of the samples, ε_0, were between 0.04 and 0.28, calculated porosities for the samples obtained at atmospheric pressure were in the range of 0.55–0.82 and under elevated pressure (only $MgCO_3$ decomposes) in the range of 0.11–0.42.

Table 3. Structural parameters of the calcined samples (L = limestone, D = dolomite)

Sample (Deposit)	ε_l	S_{vl}, m^2/cm^3	d_{av}, μm
	P = 1 bar		
Rummu L	0.820	1.36	2.41
Aseri L	0.566	8.34	0.27
Harku L	0.571	5.82	0.39
Karinu L	0.579	1.43	1.62
Tamsalu L	0.569	0.265	0.47
Volkhov L	0.554	2.64	0.84
Adavere D	0.575	0.464	4.96
Pajusi D	0.617	2.37	1.04
Koguva D	0.583	5.00	0.47
Hellamaa D	0.643	0.770	3.34
	P = 15 bar		
Rummu L	0.285	2.35	0.497
Aseri L	0.188	15.11	0.050
Harku L	0.159	11.68	0.054
Karinu L	0.113	4.06	0.111
Tamsalu L	0.185	2.15	0.344
Volkhov L	0.144	5.76	0.100
Adavere D	0.314	2.82	0.446
Pajusi D	0.420	5.74	0.292
Koguva D	0.352	17.42	0.081
Hellamaa D	0.329	7.08	0.186

The specific surface area was measured by a nitrogen adsorption method (BET method). Porosity and pore distribution as well as sorbent density measurements were carried out by the high pressure Hg intrusion method (Quantachrome Autoscan 33 porosimeter, pore size range 6.5–1500 nm). Besides, SEM and X-ray methods were used to characterize the initial materials and products obtained.

RESULTS AND DISCUSSION

The USC model [16] for constant size particles can be used for the preliminary characterization of solid–gas reactions. However, this model is

limited to the case where either kinetics or intra-particle diffusion is rate determining.

In the process of sulphur capture four different steps can be distinguished, which can be simultaneously rate determining: external mass transfer from the surrounding gas to the surface of particles (or sample holder), sample bed diffusion inside the sample holder, chemical kinetics, and diffusion inside the particle. Besides, with this kind of reactions, the structure of the sorbent particle is continuously changing as the reaction surface shifts into the particle. In this case more flexible modelling is needed.

Here, the diffusion inside the sorbent particle was taken conversion-dependent; the effective diffusivity, which covers diffusion both in the pores and in the product layer, was given as a function of conversion and structural parameters of the sorbent.

For the case when some or all these mechanisms are rate controlling, the concept of "additive reaction times" [17] can be used. According to this concept, the time to achieve a certain degree of conversion can be expressed as follows (see Notation):

$$t = \tau_{\mathrm{emt}} F_{\mathrm{emt}}(X) + \tau_{\mathrm{sbd}} F_{\mathrm{sbd}}(X) + \tau_{\mathrm{kin}} F_{\mathrm{kin}}(X) + \tau_{\mathrm{dif}} F_{\mathrm{dif}}(X). \tag{13}$$

Time scales (time necessary for complete conversion according to that mechanism) and the respective conversion functions for external mass transfer and sample bed diffusion control can be calculated from the geometry of the thermal analyser and experiment conditions [6, 15, 18]. Time scales and conversion functions for chemical kinetics control were as follows:

$$\tau_{\mathrm{kin}} = \frac{R_{\mathrm{p}} \rho_{\mathrm{mol,solid}}}{b k_{\mathrm{s}} c_{\mathrm{gas}}}, \qquad F_{\mathrm{kin}}(X) = 1 - (1 - X)^{1/3}, \tag{14}$$

and for intra-particle diffusion:

$$\tau_{\mathrm{dif}} = \frac{R_{\mathrm{p}}^2 \rho_{\mathrm{mol,solid}}}{6 b D_{\mathrm{dif}} c_{\mathrm{gas}}},$$

$$F_{\mathrm{dif}}(X) = 3\left(\frac{Z - (Z + (1 - Z)(1 - X))^{2/3}}{Z - 1} - (1 - X)^{2/3} \right) \quad \text{if} \quad Z \neq 1. \tag{15}$$

To determine the kinetics time scale a Taylor series expansion for small conversions (X) of Eq. 14 was used as described earlier by Zevenhoven et al. [14].

Variable effective diffusivity

Effective diffusivity (D_{dif}) inside the sorbent particle includes two sequential processes: diffusion in pores (D_{pore}) and diffusion through the product layer (D_{pl}), which are combined as follows:

$$\frac{Vol_{pores} + Vol_{pl}}{D_{dif}} = \frac{Vol_{pl}}{D_{pl}} + \frac{Vol_{pores}}{D_{pore}}. \tag{16}$$

Both the volume of pores and the volume of product layer change along with conversion. It was shown [13–15] that a simple equation can be derived to describe the conversion-dependent effective diffusion using two parameters A and B, where A depends only on the initial porosity of the calcined solid (ε_1) and B must be derived from a time–conversion (t–X) data set.

$$A = \frac{1-\varepsilon_1}{\varepsilon_1},$$

$$B = \frac{Z(1-\varepsilon_1)D_{mol+Kn}}{3\,D_{pl}},$$

$$D_{dif} = D_{dif,0}\frac{1+AX}{1+BX}, \tag{17}$$

$$D_{dif,0} = D_{pore,0} = D_{mol+Kn}\frac{\varepsilon_1}{\gamma},$$

$$D_{pl} = \frac{A\,Z\,D_{dif,0}}{B}.$$

Here, D_{mol+Kn} is the combined molar and Knudsen diffusivity for the reactant gas at a certain average pore radius. Tortuosity γ was taken equal to 3 in these calculations. Having determined the value for B, it is possible to calculate also the product layer diffusivity D_{pl}.

Taking into consideration the small but necessary corrections for sample bed diffusion and external mass transfer, the USC model with variable effective diffusivity can be expressed as follows:

$$t = \tau_{kin}F_{kin}(X) + \tau_{dif,0}\frac{1+BX}{1+AX}F_{dif}(X). \tag{18}$$

Parameters into this model ($\tau_{dif,0}$ and B) were found using a non-linear least squares curve fitting routine.

In order to obtain parameters into the extended USC model (i.e. with variable effective diffusivity), information on the structure of the sorbent sample (density, porosity, pore size distribution, specific surface area) and a time–conversion (t–X) data set are needed.

Sulphation data obtained at atmospheric pressure

Tests were carried out with six limestone and four dolomite samples. It can be seen (Fig. 1) that the sulphation of limestone samples started at high speed and in approximately 200–300 s up to 25–44% of $CaCO_3$ conversion was achieved. After that there was a sharp decrease in the binding rate and the final degrees of conversion at 2 h duration of the experiment were in the range of 36–54%.

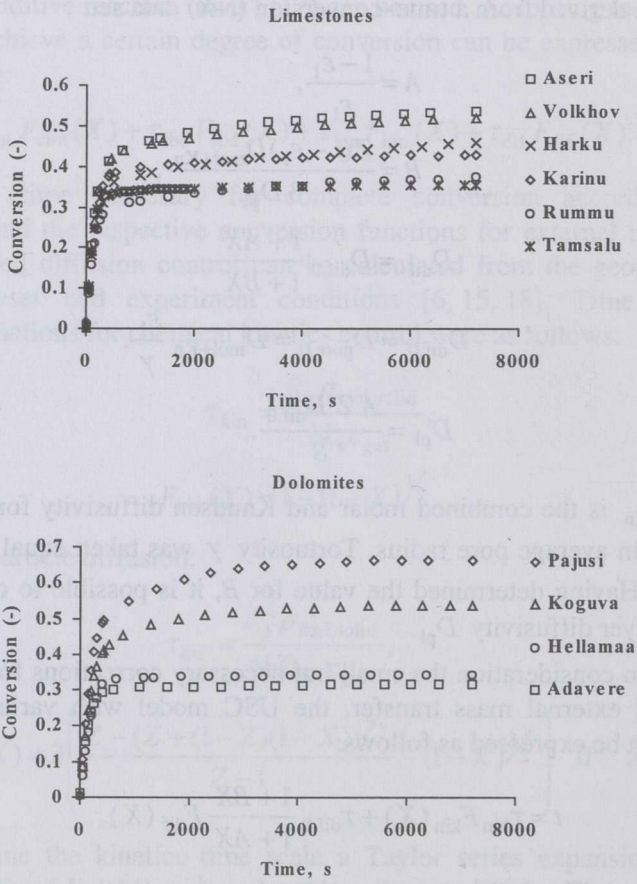

Fig. 1. Sulphation data of calcined limestones and dolomites at atmospheric pressure.

The same phenomenon was observed with the dolomite samples, the final values for conversion being in the range of 32–66%. It was determined that for some dolomite samples the degree of conversion calculated on the basis of only the chemically determined CaO content would have been over 100%. This indicated that in these conditions MgO also took part in sulphur binding. Therefore, conversion of limestone samples was calculated only on the basis of $CaCO_3$, conversion of dolomite samples on the basis of the sum of $CaCO_3$ and $MgCO_3$. X-ray measurements verified that a mixed sulphate $CaMg_3(SO_4)_4$ was present in the products.

The highest values for the degree of conversion were measured for Aseri and Volkhov limestone and Pajusi and Koguva dolomite. All these are quite impure materials, last three have a high content of insoluble residue (14–19%), and Aseri limestone has a very high Fe_2O_3 content (Table 1). The increase in the degree of conversion in 2 h experiment compared with 1 h experiment remained below 6% for several samples and it was equally low for all the dolomite samples.

Sulphation data obtained at pressurized conditions

The sorbent samples were tested also at pressurized conditions typical of in-bed sulphur capture in pressurized fluidized bed combustion. Under 15 bar pressure the sulphation of $CaCO_3$ started at a much lower speed, especially for limestone samples, but after 2–3 h of the experiment, the reaction had still a noticeable speed in most cases (Fig. 2). However, the initial sulphation rate of dolomite samples was remarkable also at pressurized conditions. The increase in the degree of conversion between 1 h and 2 h experiments was high for limestone samples (up to 25% as compared to 6% at atmospheric pressure), but low for dolomite samples.

It can be seen (Figs. 1 and 2) that for limestone samples the influence of pressurizing is noticeably higher than for dolomite samples. The effect of pressure was negligible for Adavere and Hellamaa dolomite, which had low initial porosities and small pore surface areas.

A relationship was observed between the degree of conversion and the content of insoluble residue, both at atmospheric pressure (Fig. 3) and under 15 bar pressure. The higher the content of insoluble residue, the higher was the final degree of conversion. Presumably, the impurities in the sorbent create an inert porosity structure allowing the SO_2 gas to reach the boundary of the unreacted part of the sorbent particle more easily.

Another characteristic we have been using to express the sulphur binding ability of a sorbent is binding capacity (*BC*, mg SO_2 per 100 mg of initial sample). In the experiments carried out at atmospheric pressure *BC* remained in the range of 15.5–33.9 mg/100 mg, the highest value corresponding to Pajusi

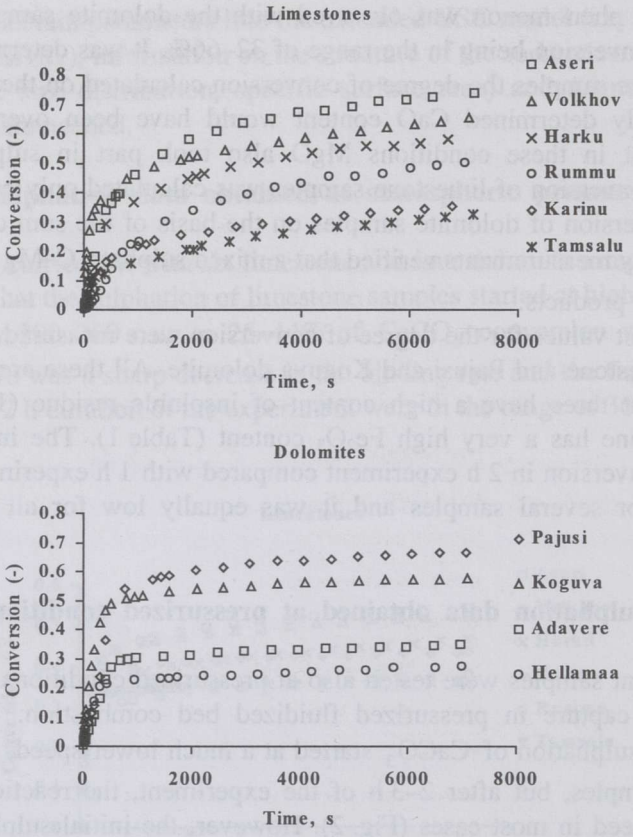

Fig. 2. Sulphation data of limestones and dolomites under 15 bar pressure.

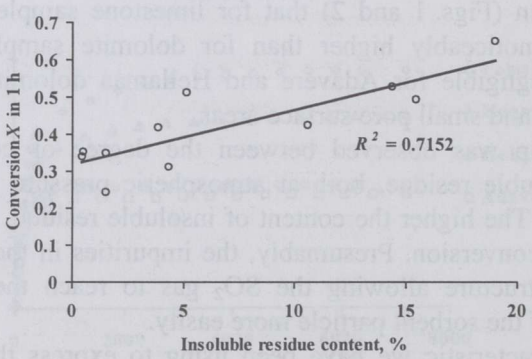

Fig. 3. Correlation between conversion during 1 h and impurities content at $P = 1$ bar.

dolomite. At pressurized conditions *BC* was in the range of 14–34 mg/100 mg, the highest value corresponding again to Pajusi dolomite. However, the highest values for the degree of conversion did not always correspond to the highest values of *BC* (Fig. 4). Besides, the values of *BC* differed less than $CaCO_3$ conversion, which means that the binding capacity of the impure samples (Pajusi D, Aseri L, Koguva D) was utilized to a greater extent.

Thus, the best results at atmospheric and pressurized experiment conditions were obtained by the use of relatively impure Pajusi and Koguva dolomite samples and by Aseri and Volkhov limestone samples. Porosities (ε_0) as well as

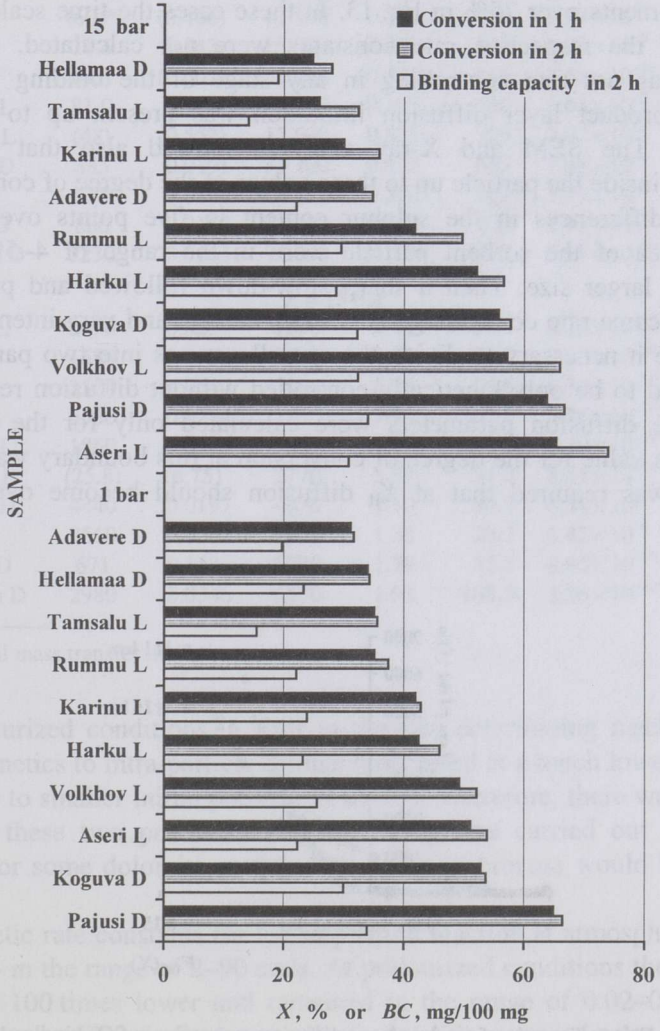

Fig. 4. Comparison of SO_2 binding ability of the sorbent samples.

pore surface areas of these samples (S_{v0}) were relatively high compared to other sorbent samples. Rummu limestone had also quite high porosity, but lower initial internal surface and its binding ability remained somewhere in the middle. The poorest results were obtained with Tamsalu limestone, its S_{v0} and S_{v1} being also relatively low.

Model calculations at atmospheric pressure

At atmospheric pressure the sulphation process started at a remarkable speed and proceeded evenly throughout the sorbent particle. The external mass transfer influenced the overall process significantly during the first 100 s, reaching in some experiments over 75% in Eq. 13. In these cases the time scale for kinetic control and the respective rate constants were not calculated. Sample bed diffusion was not rate controlling in any stage of the binding process. No noticeable product layer diffusion limitation was present up to 25–44% of conversion. The SEM and X-ray analyses showed also that the sulphur distribution inside the particle up to these values of the degree of conversion was uniform – differences in the sulphur content in five points over the cross-sectional area of the sorbent particle were in the range of 4–5%, even for particles of larger size. Then a sharp slow-down followed and product layer diffusion became rate controlling. This sharp change and very intensive starting period made it necessary to divide the overall process into two parts. The first was assumed to be only kinetically controlled without diffusion resistance and intra-particle diffusion parameters were calculated only for the second part (Fig. 5). The value for the degree of conversion at this boundary was marked as X_{II} and it was required that at X_{II} diffusion should become over 25% rate controlling.

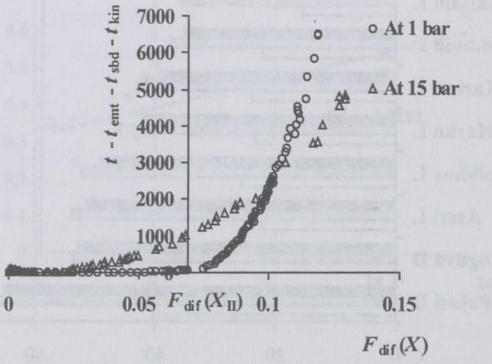

Fig. 5. The role of product layer diffusion resistance in SO_2 binding.

Modelling results are presented in Table 4. Unfortunately, there was no well established correlation between X_{II} and any physical or chemical properties of the sorbent, so X_{II} becomes a separate parameter that must be estimated on the basis of the t–X data set. In these experiments the values for X_{II} were in the range of 0.26–0.49.

Table 4. Modelling results (L = limestone, D = dolomite)

Sample (Deposit)	τ_{kin}, s	k_s, m/s	B	A	$\tau_{dif,0}$, s	D_{pl}, m^2/s	X_{II}
			P = 1 bar				
Rummu L	38.0	0.909	22 700	0.299	445	8.29×10^{-10}	0.283
Aseri L	(60)*	(0.406)	12 500	0.715	246	1.27×10^{-9}	0.405
Harku L	77.4	0.343	15 900	0.857	348	1.28×10^{-9}	0.343
Karinu L	(60)	(0.501)	51 300	0.440	986	7.67×10^{-10}	0.377
Tamsalu L	81.0	0.306	33 000	0.187	646	1.64×10^{-9}	0.299
Volkhov L	(48)	(0.552)	15 600	0.829	306	2.07×10^{-9}	0.412
Adavere D	885	0.0191	34 100	0.416	645	1.48×10^{-9}	0.258
Pajusi D	675	0.0188	8 190	0.580	161	3.73×10^{-9}	0.494
Koguva D	880	0.0169	11 200	0.644	220	1.97×10^{-9}	0.402
Hellamaa D	1230	0.0165	71 000	0.121	1340	5.61×10^{-10}	0.314
			P = 15 bar				
Rummu L	8850	0.0259	3290	2.48	39.4	8.22×10^{-10}	
Aseri L	1680	0.0958	2290	4.28	31.7	7.40×10^{-10}	
Harku L	2560	0.0687	2990	5.25	56.6	6.34×10^{-10}	
Karinu L	5530	0.0354	7840	7.70	107.5	3.26×10^{-10}	
Tamsalu L	1860	0.0771	6900	4.37	137.0	4.30×10^{-10}	
Volkhov L	(25.8)	(6.75)	2770	5.87	54.0	8.61×10^{-10}	
Adavere D	4440	0.0197	4070	2.10	80.8	6.31×10^{-10}	
Pajusi D	2560	0.0267	1450	1.35	28.2	1.42×10^{-9}	
Koguva D	671	0.118	1930	1.79	38.5	8.66×10^{-10}	
Hellamaa D	2980	0.0346	6570	1.92	108.5	3.36×10^{-10}	

* High external mass transfer limitations.

At pressurized conditions, a shift in the rate determining mechanism from chemical kinetics to intra-particle diffusion occurred at a much lower conversion (Fig. 5) due to smaller initial porosity (Table 3). Therefore, there was no need to distinguish these two processes and modelling was carried out in one step. However, for some dolomite samples the two-step process would have given a better fit.

The kinetic rate constants for the sulphation reaction at atmospheric pressure were high – in the range of 2–90 cm/s. At pressurized conditions the values of k_s were about 100 times lower and remained in the range of 0.02–0.1 cm/s. The values for the coefficient B at atmospheric conditions were in the order of 10^4, under pressure in the order of 10^3. Calculated on the basis of the coefficient B,

product layer diffusivities were in the range of $3.2 \times 10^{-10} - 3.7 \times 10^{-9}$ m^2/s and for several samples they were slightly less at pressurized conditions.

A comparison of test data and model calculations is presented in Fig. 6. It can be seen that the two-step modelling of the sulphation process at atmospheric pressure gave a good fit, but the need for the determination of X_{II} and increased manipulations with the t–X data make this approach more complicated. Presumably, finding a mean value of X_{II} for a certain group of similar samples could be reasonable.

Modelling the data obtained at pressurized conditions gave a satisfactory fit in case of limestone samples, but with the dolomite samples a more rapid shift from kinetic to diffusion control and a too steep increase in the effective diffusion resistance was assumed by the model.

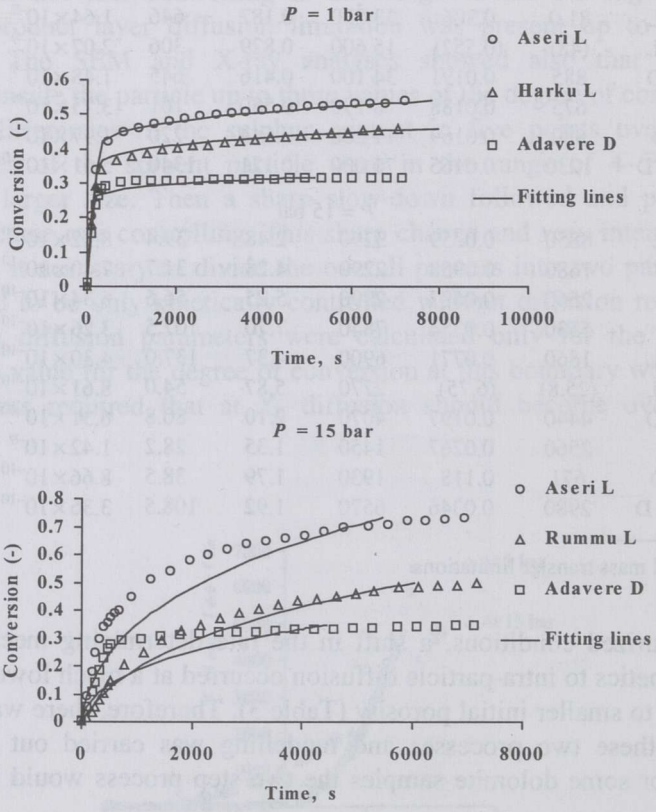

Fig. 6. Comparison of test data with model calculations.

CONCLUSIONS

It was shown that at atmospheric pressure sulphation starts at a high speed (values of the rate constants 2–90 cm/s) and in 200–300 s up to 25–44% of conversion was achieved. After that a sharp shift from chemical kinetics control to intra-particle diffusion control was observed. The values for the final degree of conversion and binding capacity at 850 °C and for 125–160 μm particles were in the range of 32–66% and 16–34 mg of SO_2 per 100 mg of initial sample, respectively. Impurities in the sorbent increased the final degree of conversion.

Under 15 bar pressure the initial sulphation rate was noticeably lower (values of the rate constants 0.02–0.1 cm/s). The shift from chemical kinetics control to diffusion control took place at remarkably lower conversion values, especially for the limestone samples. The values for the degree of conversion and binding capacity were almost in the same range. However, the increase in the degree of conversion during the second hour of experiment was remarkably higher compared to the values obtained under atmospheric pressure.

The best binding results (conversion during 1 h experiment) were obtained with samples that had high initial porosities and pore surface areas as well as a high content of impurities – Volkhov and Aseri limestone and Pajusi and Koguva dolomite samples.

The increase in the intra-particle diffusion resistance predicted by the extended USC model at atmospheric pressure was remarkably higher than in the real process. Therefore, a two-step modelling was carried out, assuming that up to a certain degree of conversion the sulphation process is not diffusion controlled. However, the USC model was successfully applied to the data obtained under pressurized conditions, especially in case of limestone samples. In several cases, especially at atmospheric conditions, external mass transfer limitations were high at the beginning of the experiment due to the extremely high reactivity of the calcined limestone, so the obtained values for the rate constants should be treated with certain caution.

Extending the studies to estimate the influence of other controllable parameters such as temperature, O_2 concentration, particle size, etc. could be useful to create a basis for selecting the best sorbents from different calcareous rocks.

ACKNOWLEDGEMENTS

The authors would like to thank Mikko Hupa for valuable discussions, Peter Backman for his help in the TG experiments, and Helgi Veskimäe for carrying out chemical analyses.

NOTATION

A, B	dimensionless parameters in the extended USC model	–
b	stoichiometric coefficient in the sulphation reaction	–
BC	SO_2 binding capacity (mg of bound SO_2 per 100 mg of initial sample)	mg/100 mg
c_{gas}	SO_2 concentration in bulk gas	mol/m^3
d_{av}	average diameter of the pores	m
D_{dif}	effective intra-particle diffusivity	m^2/s
D_{mol+Kn}	combined molar and Knudsen diffusivity	m^2/s
D_{pl}	product layer diffusivity	m^2/s
D_{pore}	diffusivity in pores	m^2/s
$F(X)$	conversion function for a definite mechanism: dif intra-particle diffusion; emt external mass transfer; kin chemical kinetics; sbd sample bed diffusion	
k_s	reaction rate constant	m/s
r_{av}	average radius of the pores	m
R_p	sorbent particle radius	m
S_{v0}	pore surface area of raw sorbent particle	m^2/m^3
S_{v1}	pore surface area of calcined sorbent	m^2/m^3
Z	molar volume ratio of solid product and reactant ($V_{CaSO_4}/V_{CaO} = 2.72$, $V_{CaSO_4}/V_{CaCO_3} = 1.25$)	–
t	time to achieve conversion X	s
Vol_{pl}	volume of product layer	m^3
Vol_{pores}	volume of pores	m^3
$Vol_{pores,0}$	volume of pores of the initial sample	m^3
$Vol_{pores,1}$	volume of pores of the calcined sample	m^3
X	degree of conversion	–
X_{II}	degree of conversion at which intra-particle diffusion becomes dominant	–
ε_0	initial porosity of raw sorbent particle	m^3/m^3
ε_1	initial porosity of calcined sorbent particle	m^3/m^3
$\rho_{mol,solid}$	molar density of solid reactant	mol/m^3
$\rho_{particle}$	density of sorbent particle	kg/m^3
$\rho_{CaCO_3, MgCO_3}$	density of pure $CaCO_3$ or $MgCO_3$	kg/m^3
γ	tortuosity ($\gamma = 3$)	–
τ_{dif}	intra-particle diffusion time scale	s
τ_{emt}	external mass transfer time scale	s
τ_{kin}	chemical kinetics time scale	s
τ_{sbd}	sample bed diffusion time scale	s
$\%CaCO_3$	$CaCO_3$ content in the sample	%
$\%MgCO_3$	$MgCO_3$ content in the sample	%

REFERENCES

1. *Estonian Environment 1996*. Estonian Environment Information Centre, Tallinn, 1997.
2. Kaljuvee, T., Trikkel, A. & Kuusik, R. Comparative reactivity of some calcareous rocks as sorbents towards sulphur dioxide. *Proc. Estonian Acad. Sci. Chem.*, 1994, **43**, 146–156.
3. Iisa, K., Hupa, M. & Yrjas, P. Product layer diffusion in the sulphation of calcium carbonate. In *Proc. of the Twenty-Fourth International Symposium on Combustion, Sydney, Australia, July 5–10.* 1992, 943–948.
4. Borgwardt, R. H., Bruce, K. R. & Blake, J. An investigation of product-layer diffusivity for CaO sulfation. *Ind. Eng. Chem. Res.*, 1987, **26**, 1993–1998.
5. Tullin, C., Nyman, G. & Ghardashkhani, S. Direct sulfation of $CaCO_3$: The influence of CO_2 partial pressure. *Energy Fuels,* 1993, **7**, 512–519.
6. Iisa, K. & Hupa, M. Rate-limiting process for the desulphurisation reaction at elevated pressures. *J. Inst. Energy*, 1992, **65**, 201–205.
7. Chan, R. K., Murthi, K. S. & Harrison, D. Thermogravimetric analysis of Ontario limestones and dolomites I. Calcination, surface area, and porosity. *Can. J. Chem.*, 1970, **48**, 2972–2978.
8. Schwitzgebel, K. & Lowell, P. S. Thermodynamic basis for existing experimental data in Mg–SO_2–O_2 and Ca–SO_2–O_2 systems. *Environ. Sci. Technol.*, 1973, **7**, 1147–1151.
9. Petersen, E. E. Reaction of porous solids. *AIChE J.*, 1957, **3**, 443–448.
10. Szekely, J. & Evans, J. W. A structural model for gas–solid reactions with a moving boundary. *Chem. Eng. Sci.*, 1970, **25**, 1091–1107.
11. Bhatia, S. K. & Perlmutter, D. D. The effect of pore structure on fluid–solid reactions: Application to the SO_2 – lime reaction. *AIChE J.*, 1981, **27**, 226–234.
12. Alvfors, P. & Svedberg, G. Modeling of the sulphation of calcined limestone and dolomite – a gas-solid reaction with structural changes in the presence of inert solids. *Chem. Eng. Sci.*, 1988, **43**, 1183–1193.
13. Zevenhoven, R., Yrjas, P. & Hupa, M. Sulfur dioxide capture under PFBC conditions: The influence of sorbent particle structure. *Fuel*, 1998, **77**, 285–292.
14. Zevenhoven, C. A. P., Yrjas, K. P. & Hupa, M. M. Hydrogen sulfide capture by limestone and dolomite at elevated pressure. 2. Sorbent particle conversion modeling. *Ind. Eng. Chem. Res.*, 1996, **35**, 943–949.
15. Trikkel, A., Zevenhoven, R. & Kuusik, R. Estonian calcareous rocks as SO_2 sorbents in AFBC and PFBC conditions. In *15th International Conference on Fluidized Bed Combustion, May 9–13 1999. Savannah, Georgia, USA: Proceedings on CD-ROM.*
16. Levenspiel, O. *Chemical Reaction Engineering*. Wiley, New York, 1972.
17. Sohn, H. Y. The law of additive reaction times in fluid–solid reactions. *Metall. Trans. Bull.*, 1978, **9B**, 89–96.
18. Iisa, K., Tullin, C. & Hupa, M. Simultaneous sulfation and recarbonation of calcined limestone under PFBC conditions. In *11th International Conference on Fluidized Bed Combustion. Proceedings.* American Society of Mechanical Engineers, 1991, ASME Book No. 10312A, 83–90.

EESTI LUBJAKIVIDE JA DOLOMIITIDE SO_2 SIDUMISE MODELLEERIMINE

Andres TRIKKEL, Ron ZEVENHOVEN ja Rein KUUSIK

On uuritud keemiliselt koostiselt ja struktuuriomadustelt erinevate Eesti lubjakivide ning dolomiitide SO_2 sidumise iseärasusi atmosfäärirõhul ning rõhu all kulgevas protsessis, kasutades termogravimeetrilist ja röntgendifraktsioonanalüüsi, skaneerivat elektronmikroskoopiat ning kõrgrõhu elavhõbeda porosimeetriat. SO_2 sidumine toimus isotermiliselt temperatuuril 850 °C, rõhul 1 bar või 15 bar, gaasikeskkonnas, mis sisaldas 4% O_2, 15% CO_2, 0,5% SO_2 ja lämmastikku. Katsetulemuste matemaatilise töötlemise aluseks oli reageerimata kahaneva sfääri mudel, mida täiendati konversioonsõltuva efektiivse difusiooni sisseviimisega. Atmosfäärirõhul, kus eelnevalt lagunenud materjal seob SO_2, on reaktsioon algfaasis kiire ning olulist produktikihi difusioonitakistust konversiooniastmeteni 25–44% ei esine. Seejärel kasvab difusioonitakistus järsult. Rõhu all toimuvas protsessis on SO_2 sidumine algfaasis oluliselt aeglasem ning üleminek difusioonitakistuse piirkonda toimub madalamatel konversiooniastmetel. Konversiooniastmete väärtused jäävad 2-tunnise katseaja lõpuks vahemikku 32–66% ja SO_2 sidumisastmed vahemikku 15,5–34 mg SO_2 100 mg algmaterjali kohta. Atmosfäärirõhul toimuva SO_2 sidumise modelleerimist on otstarbekas teha kahes astmes, arvestades esimeses vaid keemilise reaktsiooni kiiruse limiteerivat mõju, teises difusioonitakistuse mõju. Rõhu all toimuva sidumise kirjeldamiseks kasutati mudelit üheastmelisena.